Available online at www.sciencedirect.com
ScienceDirect
Ceramics International 36 (2010) 93–101
CERAMICS INTERNATIONAL
www.elsevier.com/locate/ceramint

A new technological procedure using sucrose as porogen compound to manufacture porous biphasic calcium phosphate ceramics of appropriate micro- and macrostructure

A.-M. Le Ray [a,*], H. Gautier [b], J.-M. Bouler [b], P. Weiss [b], C. Merle [b]

[a] Université d'Angers, Laboratoire SONAS, IFR 149 Quasav, 16 Boulevard Daviers, 49100 Angers, France
[b] Université de Nantes, Laboratoire LIOAD, INSERM U 791, 1 Place Alexis Ricordeau, 44042 Nantes, France

Received 6 April 2009; received in revised form 11 June 2009; accepted 1 July 2009
Available online 17 July 2009

Abstract

In the domain of implantable materials, the porosity and pore size distribution of a material in contact with bone is decisive for bone ingrowth and thus the control of the porosity is of great interest. The use of a new porogen agent, *i.e.* sucrose is proposed to create a porosity in biphasic calcium phosphate blocks. The technological procedure is as follows: sucrose and mineral powder are mixed, then compressed by isostatic compression and sintering finally eliminates sucrose. Blocks obtained were compared to a manufactured product: Triosite® (Zimmer, Etupes, France) which porosity is created through a naphthalene sublimation process.

Results have shown that the incorporation of sucrose allows the preparation of porous blocks with controlled porosity varying from 40 to 80% and with macro-, meso- and microporosity characteristics depending on the percentage of sucrose added as well as on the granulometry of both sucrose and mineral powder.

Keywords: B. Porosity; B. Electron microscopy; Mercury porosimetry; Calcium phosphate ceramics

1. Introduction

Due to their chemical composition close to the bone mineral (biological apatite), the main bioactive ceramics used for implants are calcium phosphate ceramics (CaP). The efficiency of such CaP ceramics is related to their chemical nature as well as to their porous structure. To be invaded by bone ingrowth and to allow body fluid circulation, the CaP ceramics have to be porous (total pore volume near 60%), *i.e.* they must contain both macropores of at least 100 μm – most of them lying between 150 and 300 μm – and micropores inferior to 5–10 μm, this last fraction being not greater than 5–10% [1–10]. Therefore, control of porosity within the porous bioceramics is a critical matter. Another problem for these porous structures is their low compression strength and modulus, which are quite different from those exhibited by cancellous bone [10–13].

Many processes have been described for the preparation of porous materials: use of replica sponge structures such as the so-called polymeric sponges (reticulate ceramics) [10,14–16] followed by heat treating, replicas of marine coral [17]; introduction of porogen substances which will create a porous structure after calcination and which integrity is maintained through the sintering step (naphthalene particles [18,19]), organic polymers such as poly vinyl butyral (PVB) [7,20], polystyrene or polymethyl methacrylate beads [6], sodium chloride grains [21], calcium polyphosphate particles [22], cellulosic powder or artificial polymers and binders [11], flour [23], gas-forming (carbon dioxide, hydrogen) agent such as ball-shaped granules of clay (foam ceramics) [14], $CaCo_3$ [24,25], hydrogen peroxide [5] and so on. However, each technique has its own limit: relatively low strength (polymeric sponges, cellulosic powder or artificial polymers and binders), pore size limited to several micrometers ($CaCo_3$, flour), or low permeability in foam ceramics (open and closed voids) when compared to reticulate ceramics (interconnected voids) [14].

* Corresponding author at: Laboratoire SONAS, UFR des Sciences Pharmaceutiques et Ingénierie de la Santé, 16 Boulevard Daviers, 49000 Angers, France. Tel.: +33 02 41 22 66 65; fax: +33 02 41 48 67 33.
E-mail address: anne-marie.leray@univ-angers.fr (A.M. Le Ray).

0272-8842/$36.00
doi:10.1016/j.ceramint.2009.07.001

We have already shown [4,26,27] that porous blocks of biphasic calcium phosphate (BCP) with a macroporosity close to 50% (mean pore size of 400–600 μm), a microporosity of about 35% and a 60/40 hydroxyapatite (HA)/tricalcium phosphate β (β-TCP) ratio have a degradation rate adapted to bone ingrowth kinetics. The method employed to create the porosity of these blocks is the Hubbard's one [18], where 50% of calibrated naphthalene particles (mean: 500 μm) were added to 80–200 μm mixed powders of HA and β-TCP. Samples were subjected to isostatic compression (200 MPa) and the resulting blocks were sintered at 1100 °C, after being subjected to a slow thermal ramp (up to 550 °C) in order to eliminate the naphthalene particles by sublimation. However, this method suffers from several drawbacks such as toxicity associated to PAHs, fire setting, air pollution and difficulties of naphthalene grinding and sieving.

The aim of the present study was to test the feasibility of elaborating blocks with a controlled porosity using sucrose particles with different size fractions of 565, 407.5, 257.5 and 150 μm as the porogen agent, the sucrose being associated to the apatite powder at concentration ranging from 35 to 55% (v/v). This compound is cheaper, safer and easier to manipulate than naphthalene. Resulting powder mixtures were submitted to high pressure using isostatic compression, and then sintered. Porosity and pore size distribution were evaluated through scanning electron microscopy (SEM) coupled to image analysis and through mercury porosimetry. Blocks were compared with ceramics obtained after sublimation of naphthalene as the porogen agent [18].

2. Experimental procedures

2.1. Materials

The synthesis of the calcium deficient apatite (CDA) was completed by alkaline hydrolysis of dicalcium phosphate dehydrated (DCPD, Merck, France) [28]. Crystalline sucrose (Beghin Say, France), used as the porogen compound, was previously mechanically sieved (503 502 Sieve, Fristch Laborgerätebau, Germany) on 630, 500, 315, 200 and 100 μm sievers for 20 min to collect 565, 407.5, 257.5 and 150 μm grains. CDA granules were obtained as follows: The CDA powder was introduced in an elastomer mold under vacuum, then the mold was transferred into a high-pressure chamber containing water and subjected to isostatic compression under 200 MPa during 2 min according to a protocol previously described [29]. Briefly, the pressure was increased to 200 MPa (3.4 MPa s^{-1}) for 2 min, then slowly decreased (1.2 MPa s^{-1}) to the atmospheric pressure using an hyperbar equipment (Alstom, Nantes, France).

The resulting compressed blocks of CDA were sintered in a controlled-temperature Vecstar furnace (Vecstar, Eurotherm, Suisse) according to the following process. The temperature was first raised to 180 °C (2 °C min^{-1}) for 240 min, then to 560 °C for 300 min in order to eliminate sugar particles, and finally to 1050 °C (3 °C min^{-1}) for 300 min. Then the blocks were cooled down to 25 °C (3 °C min^{-1}), crushed in a grooved roller breaker (TG2S, Erweka Apparatebau GmbH, Germany) and mechanically sieved for 20 min to collect 565, 407.5, 257.5 and 150 μm granules.

2.2. Block formulation

Two experimental studies were performed in parallel. In the first one, different percentages of sucrose: 35, 45 and 55% (v/v) of each granulometry (565, 407.5, 257.5 and 150 μm) were added to 65, 55 and 45% (v/v) of the synthetic CDA powder (samples 1–12), respectively. In the second one, 45% (v/v) of sucrose granules were added to 55% of CDA granules, each having the same granulometry (565, 407.5, 257.5 or 150 μm) (samples 13–16). The mixing (weight: around 80 g) were elaborated using a Turbula® (T2C, WAB, Suisse) for 3× 5 min. Each mixing was conditioned in an elastomer mold under vacuum. The mold was then isostatically compressed in a hyperbar equipment. The resulting compressed blocks of CDA and porogen were sintered in a controlled-temperature Vecstar furnace (Vecstar, Eurotherm, Switzerland). These two last operations were conducted according to the aforementioned process (see Section 2.1). Smaller blocks were then sectioned in the central region of the compressed blocks in 5 mm × 5 mm × 5 mm blocks with a diamond saw (Dremel Moto-Flex 732-T1, USA).

2.3. Physicochemical characterization

CDA purity was checked by Fourier transformed Infrared spectroscopy (Nicolet Magnat II 550 FTIR spectrometer, Paris, France) and X-ray diffraction (PW 1730 Diffractometer, Philips, France) [30,31] after sintering at 1050 °C for 5 h in the Vecstar furnace.

2.4. Morphological aspect of porous block

The blocks were embedded in a methylmetacrylate resin using the following protocol: a dehydration step (1 day in ethanol 80% (v/v), 1 day in ethanol 95% (v/v), then 1 day in absolute ethanol) was followed by an impregnation one (1 day in a mixture of absolute ethanol/methylmetacrylate: 1/1, 2 days in destabilised methylmetacrylate and 2 days in methylmetacrylate) and finally a drying step (1 week in an oven at a progressively increasing temperature: 30–80 °C). The impregnated samples were then transversally sectioned in two parts, with a diamond disc (Isomet, type 111180, low speed saw, Buehler, USA). Internal surfaces were polished with a diamond paste to achieve less than 1 μm of roughness. The two surfaces of each sample were then metallised by cathodic pulverisation (Emscope, AEI 230, Ashford, UK) with a gold–palladium complex under a 15 kV voltage (15 min), before SEM analysis (JSM-6300, Jeol, Tokyo, Japan). In those conditions, porous areas appeared in black whereas biomaterial areas varied from white to grey.

2.5. Porosity evaluation

Two methods were performed to evaluate the block porosity. In the first one, SEM was coupled to a semi-automatic image

analyser (Quantimet 500, Leica, Cambridge, UK) which allowed to evaluate the percentage of macroporosity (Ma) (>80 μm) in term of surface. The total surface of the sample was analysed and the macroporosity percentage was calculated as (porous surface/sample surface) × 100. Results were expressed as the mean percentage of 3 blocks ($n = 6$ surfaces). For the reference (Triosite®), 10 samples were similarly analysed ($n = 20$ surfaces). In the second method, *i.e.* Hg porosimetry (Autopore III 9400, Micromeritics, Creil, France), it was possible to evaluate the total porosity of the blocks (30 Å to 330 μm) expressed in term of porous volume/total volume. Classes of pores were sorted in: macroporosity (100–330 μm), mesoporosity (Me) (10–100 μm) and microporosity (Mi) (30 Å to 10 μm). Porosity percentages were evaluated in volume, by intrusion of mercury in the porous canalicules of the blocks. Results were expressed as the mean percentage of 3 blocks ($n = 3$ volumes) in each class of size. Three blocks of the commercialised product (Triosite®) were used as the control and analysed in the same conditions. Porosity results were graphically expressed in terms of total porosity, Ma, Me and Mi porosity.

3. Results

3.1. Physicochemical characterization

The IR spectra showed the typical absorptions of BCP whereas no valence vibrations could be associated neither to carbonate nor to pyrophosphate. XRD profiles of BCP powders showed peaks corresponding to BCP, allowing the two phases namely hydroxyapatite (HA) and beta tricalcium phosphate (β-TCP) to be clearly identified. The HA/β-TCP ratio was 27/73, corresponding to a Ca/P ratio of 1.62.

3.2. Morphological aspect of porous block

Morphological aspect of the porous blocks elaborated by CDA powder/sucrose granules mixing is shown in Fig. 1. When 150 and 257.5 μm granules of sucrose were added, the mixing was not homogeneous when compared with the use of 407.5 and 565 μm granules of sucrose. Morphological aspect of the porous blocks elaborated by CDA granules/sucrose granules mixing is shown in Fig. 2. Whatever the granulometry of both CDA and sucrose, the repartition of the porosity in the blocks was homogeneous.

3.3. Porosity evaluated by mercury porosimetry

3.3.1. Total porosity percentages (Fig. 3)

The total porosity percentage obtained for the reference was 68.81 ± 5.30%. When CDA powder (P) was mixed to sucrose granules (G): (P/G: 1–12), all samples presented a total porosity percentage superior to 52% [from 52.31 ± 3.11 (sample 7) to 81.18 ± 6.84% (sample 6)]. When CDA granules were mixed to 45% of sucrose granules (G/G: 13–16), the porosity percentages varied from 38.09 ± 3.14% (sample 13) to 55.34 ± 4.02% (sample 16) and were always inferior to those obtained when 45% of sucrose granules were mixed to CDA

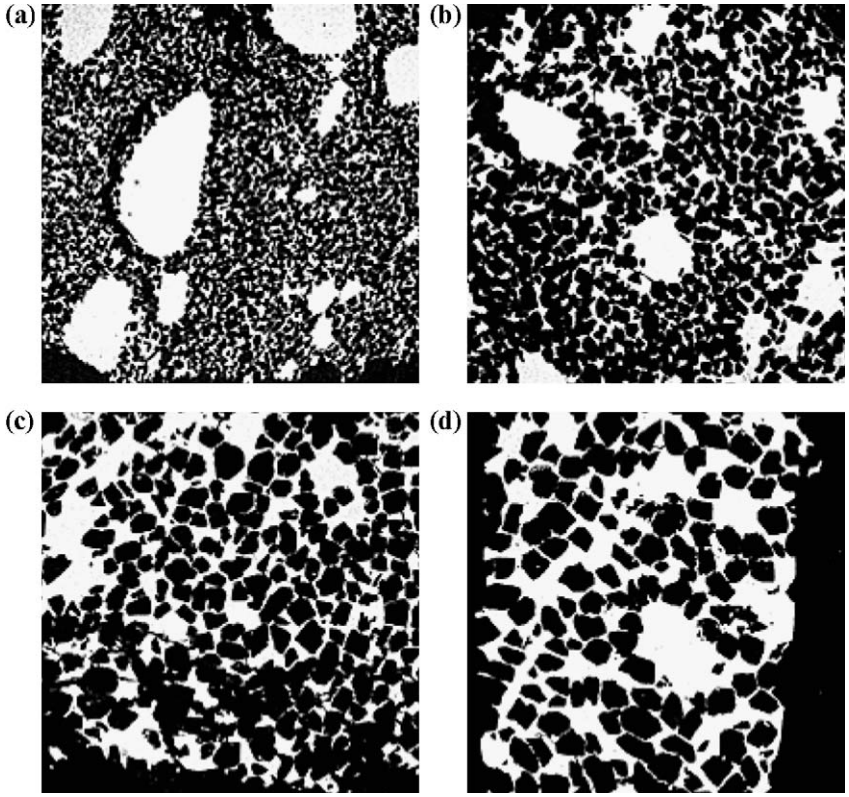

Fig. 1. SEM photographies (15×), after mixing of CDA powder with 55% of sucrose grains: (a) 150 μm, (b) 257.5 μm, (c) 407.5 μm and (d) 565 μm.

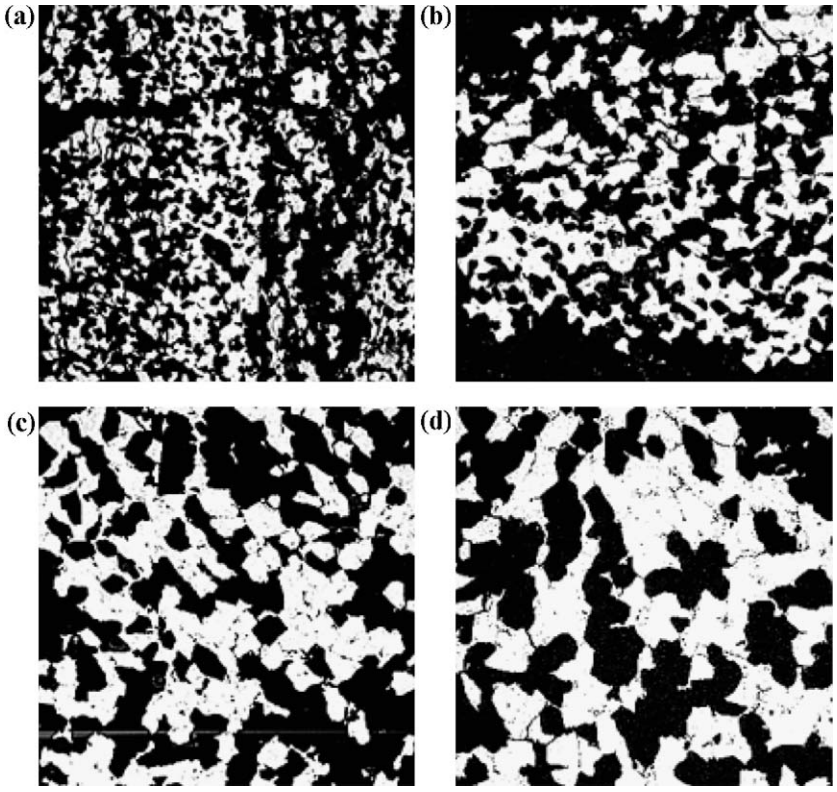

Fig. 2. SEM photographies (15×), after mixing of CDA grains with 45% of sucrose grains: (a) 150 μm, (b) 257.5 μm, (c) 407.5 μm and (d) 565 μm.

powder. Four samples exhibited a porosity close to or above the reference one: 3 (69.97 ± 7.73%), 6 (81.18 ± 6.84%), 9 (65.34 ± 4.88%) and 12 (67.61 ± 4.06%). The production of sample 6 was not constant since a lot of samples were broken and could not be analysed.

3.3.2. Macroporosity (Fig. 4)

The macroporosity percentage obtained for the reference was 8.77 ± 2.09%. When CDA powder was mixed to sucrose granules (P/G), macroporosity percentages varied from 3.40 ± 0.25 (sample 11) to 28.92 ± 1.84% (sample 3). When CDA granules were mixed to 45% of sucrose granules (G/G), the macroporosity percentages varied from 16.95 ± 6.51% (sample 16) to 27.94 ± 5.27% (sample 14) and were always superior to those obtained when 45% of sucrose granules were mixed to CDA powder. Ten samples showed a porosity close or superior to the reference: 1 (9.31 ± 2.67%), 2 (11.92 ± 3.94%), 3 (28.92 ± 1.84%), 6 (13.42 ± 3.81%), 8 (8.68 ± 5.91%), 9 (14.50 ± 3.00%) and the fourth G/G: 13 (21.12 ± 2.75%), 14 (27.94 ± 5.27%), 15 (26.32 ± 0.21%) and 16 (16.95 ± 6.51%).

3.3.3. Mesoporosity (Fig. 5)

The mesoporosity percentage obtained for the reference was 9.75 ± 4.97%. When CDA powder was mixed to sucrose granules (P/G), mesoporosity percentages varied from 19.73 ± 1.12 (sample 10) to 51.31 ± 2.43% (sample 6) and were always superior to the reference. When CDA granules were mixed to 45% of sucrose granules (G/G), mesoporosity percentages varied from 2.49 ± 0.59% (sample 13) to 25.3 ± 3.94% (sample 16). Three samples had a mesoporosity inferior to the reference (samples 13–15) and all mesoporosity percentages were always inferior to those obtained when 45% of sucrose granules were mixed to CDA powder.

3.3.4. Microporosity (Fig. 6)

The microporosity percentage obtained for the reference was 50.58 ± 5.53%. When CDA powder was mixed to sucrose granules (P/G), microporosity percentages varied from 12.07 ± 1.62 (sample 12) to 33.33 ± 2.15% (sample 10). When CDA granules were mixed to 45% of sucrose granules (G/G), the microporosity percentages varied from 12.33 ± 2.50% sample 16) to 14.61 ± 1.27% (sample 13) and were always inferior to those obtained when 45% of sucrose granules were mixed to CDA powder. Microporosity percentages were always inferior to the reference in both cases (CDA powder/sucrose granules mixing and CDA granules mixed to sucrose granules).

3.4. Macroporosity evaluated by SEM (Fig. 7)

The macroporosity percentage obtained for the reference was 48.03 ± 0.76%. When CDA powder was mixed to sucrose granules (P/G), macroporosity percentages varied from 35.08 ± 3.32% (sample 1) to 60.39% (sample 9). When CDA granules were mixed to 45% of sucrose granules (G/G), the macroporosity percentages varied from 51.25 ± 3.31% (sample 14) to 57.40 ± 2.06% (sample 16). Macroporosity percentages were superior to those obtained when 45% of sucrose granules were mixed to CDA powder for samples 13, 15 and 16. Macroporosity percentages were superior to the

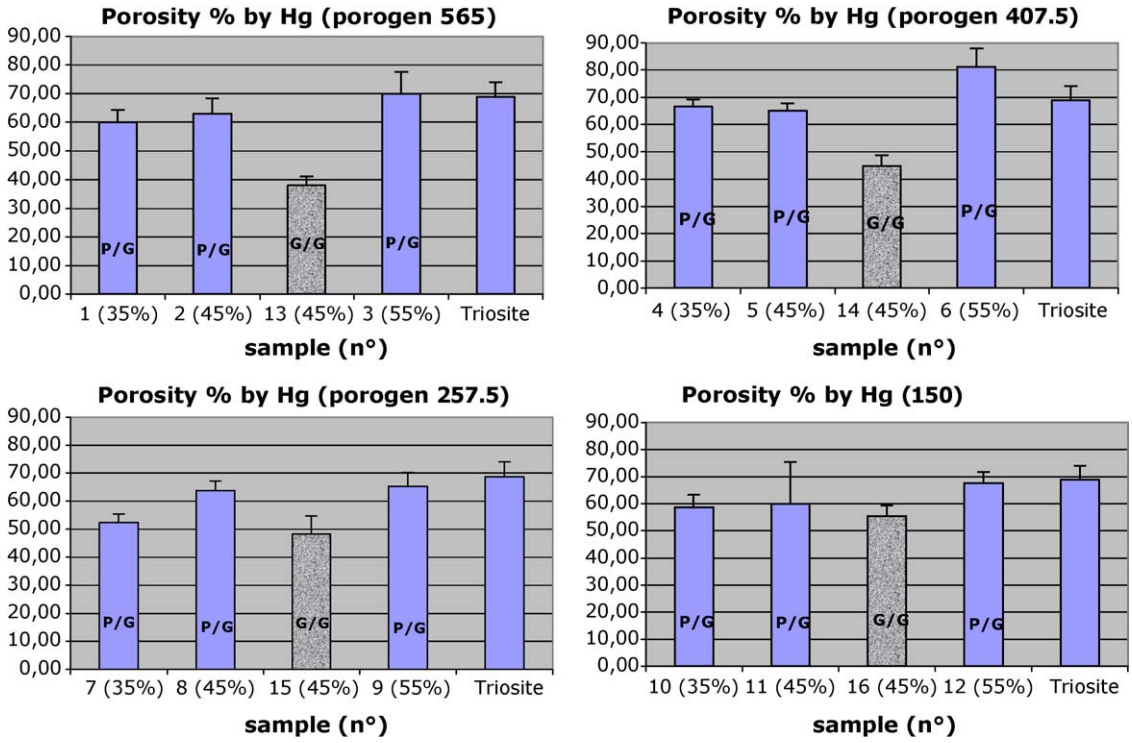

Fig. 3. Illustration of total porosity percentages obtained by Hg porosimetry for blocks 1–12 (powder/grains) and 13–16 (grains/grains).

reference for 6 samples: 3, 5, 6, 8, 9 and 12 in the case of CDA powder/sucrose granules mixing and for all samples: 13–16 in the case of CDA granules mixed to sucrose granules.

4. Discussion

The main objective of this work was to study the possibility of controlling the porosity of CaP ceramics. Different mixing of

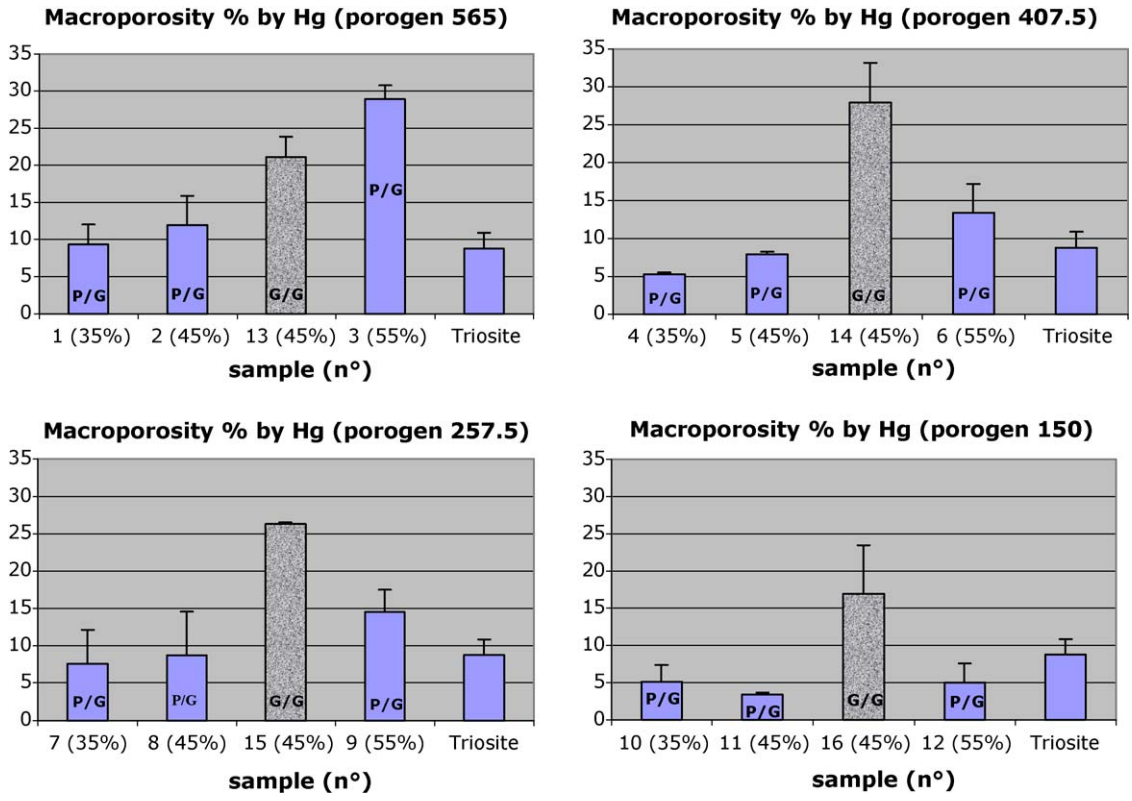

Fig. 4. Illustration of macroporosity obtained by Hg porosimetry for blocks 1–12 (powder/grains) and 13–16 (grains/grains).

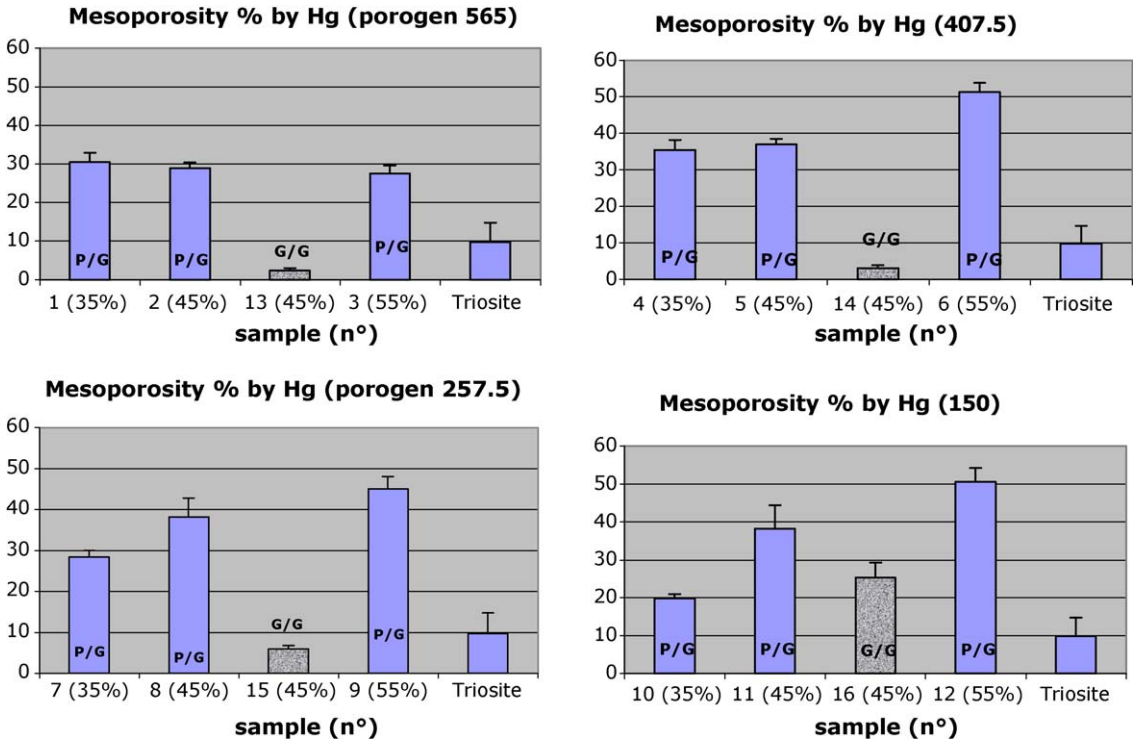

Fig. 5. Illustration of mesoporosity obtained by Hg porosimetry for blocks 1–12 (powder/grains) and 13–6 (grains/grains).

CDA and sucrose were prepared, shaped by isostatic compression, then sintered at 1050 °C. The effect of granulometry, percentage and state (powder or granule) of porogen and CDA on the porosity percentages were studied.

The porosity was evaluated using two analytical methods, *i.e.* scanning electron microscopy (SEM) and Hg porosimetry. On one hand, SEM is mainly adapted to a surface evaluation of the macroporosity (>80 μm) but is time-consuming. On the other hand Hg porosimetry is well adapted to the evaluation of the total porosity as a volume; macroporosity, mesoporosity and microporosity thus could be calculated. Samples were directly introduced in the porosimeter without any preparation, leading

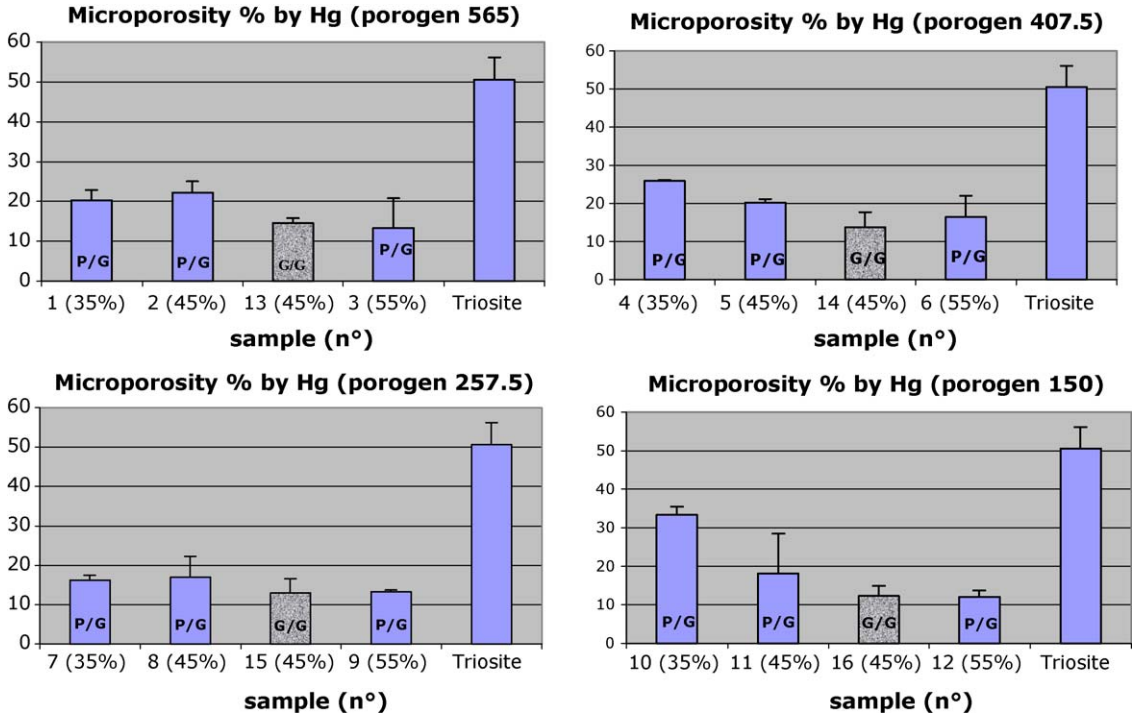

Fig. 6. Illustration of macroporosity obtained by Hg porosimetry for blocks 1–12 (powder/grains) and 13–6 (grains/grains).

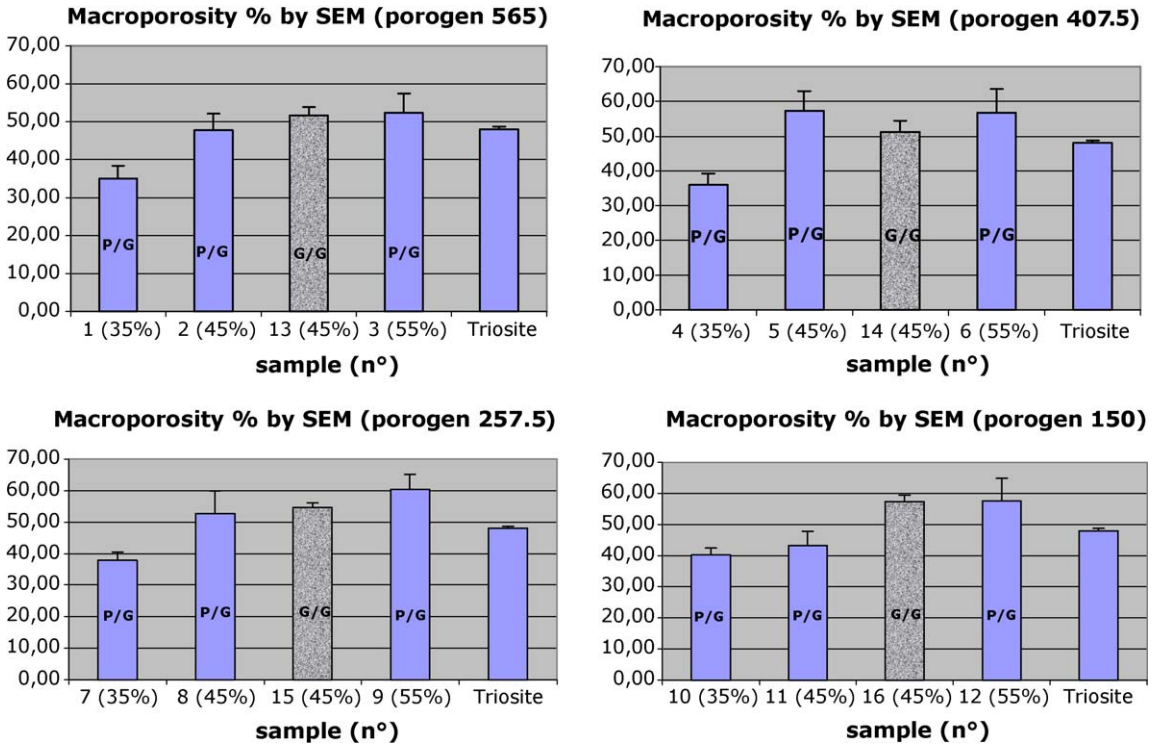

Fig. 7. Illustration of macroporosity obtained by SEM for blocks 1–12 (powder/grains) and 13–16 (grains/grains).

to pore size measurements in the 30 Å to 330 μm range. Each method gave its own informations regarding surfaces, volumes and analytical ranges. So, as formerly discussed [19], it seemed interesting to investigate them both in order to complete our analysis of the porosity.

The elaboration of the material was made according to carefully chosen experimental conditions. Indeed, the mixing time of the porogen and the mineral powder in a turbula for 3× 5 min is classical in pharmaceutical technology and allows to obtain a good powder homogeneity. The granulometry of sucrose and apatite is related to the calibrated siever: 565, 407.5, 257.5 and 150 μm. The densification of the CDA powder using the cold isostatic compression was preferred to the uniaxial pressure, since whenever the pressure is equal in all directions, maximal densification of the powders is reached leading to the obtained blocks exhibiting an homogeneous resistance [5,19]. The pressure of 200 MPa used for the isostatic compression to elaborate phosphocalcic ceramics was also validated in previous publications [29,32]. However others authors work with pressures inferior to 200 MPa [12,13,24,32], for Hubbard a pressure above 150 MPa does not give any better mechanical properties [18], while others work at pressures higher than 300 MPa [19,23].

The choice of our thermal treatment protocol was based on different criteria chosen as follows. The first criterion is the thermic degradation of the porogen [4,6,7,14,20,24,25] since its elimination creates the macroporosity. The temperature of 180 °C corresponds to the fusion of the sucrose. The porogen liquefaction induced a significant decrease of the pressure exerced onto the ceramic. The liquid can diffuse in all minerals during this first step (240 min) to create canalicules (vessels) in the whole network. The second step (560° C for 300 min) is necessary to get rid of the calcination residues of the sucrose particles or other volatil compounds. The temperature must be slowly increased to allow the polymer beads to melt and vaporize, then resulting in interconnected pores [6]. In order to minimize the potential for cracking due to the gas pressure build up and to ensure complete combustion of all polymers, a minimal hold-time of 2 h is generally chosen [24,25]. The second criterion was the physicochemical properties of the obtained ceramic. An adapted high sintering temperature was chosen in order to obtain the consolidation of the ceramic network, the densification of the macropores walls [19], the best mechanical characteristics [3] and the microporosity corresponding to the BCP interparticular spaces. Depending on the nature of calcic minerals, different temperatures [4,6,19,23], and sintering times [7,20] were described in the literature. A third step (1050 °C, 300 min) was then chosen to densify the ceramic powder. This thermal treatment protocol permitted to create porous ceramics without altering their properties.

SEM imaging clearly revealed that samples prepared by the mixing of grains/grains sharing the same granulometry, have the better porosity repartition and thus the best homogeneity compared to samples prepared by mixing of CDA powder with, respectively, sucrose grains of 565, 407.5, 257.5 and 150 μm diameters.

As far as the porosity results are concerned, the reference used in this work (Triosite®) presents a high total porosity of 69% (Hg) with the following repartition: 9% of macroporosity, 10% of mesoporosity and 51% of microporosity if referred to Hg results and 48% of macroporosity by SEM. When CDA was

added to sucrose at the powder state, it was demonstrated that the total porosity percentages obtained by Hg porosimetry increased (from 52 to 81%) with the volume percentage of porogen. This was already confirmed by other teams who determined that the total porosity depend on several parameters such as the amount of (more precisely the space occupied by) the added pore-creating medium, the temperature of sintering and the powder size [23,25]. Compared to the different percentages of total porosity described in the literature, values around 50% were often evocated [6,19] with a maximum of 62% claimed by Arita *et al.* [25]. When 45% of sucrose granules were added to CDA granules, the porosity percentages were inferior as they were comprised between 38 (sample 13, 565 μm) and 55% (sample 16, 150 μm). The best percentage of macroporosity (Hg) was obtained for sample 3 (29%) elaborated with the higher percentage (55%) of the greater sucrose granules (565 μm). When 45% of sucrose granules were added to CDA granules, two samples presented interesting macroporosity percentages (Hg): sample 14 (28%) and 15 (26%). These percentages were largely superior to the reference (9%). When the macroporosity was evaluated by SEM, the values were incomparably higher (from 35 to 60%) almost reaching the theoretical values of the introduced porogen (35, 45 and 55%). Apart from one sample where 35% of sucrose were added to the apatite, the other ones exhibited closed or higher macroporosity percentages than the reference (48%). This result was very promising as it confirmed the fact that the porogen was responsible for the created macroporosity. It also pointed to the SEM technique as the best way to evaluate the macroporosity in spite the fact that connected and non-interconnected pores were not distinguished. Anyway, if it may be considered that a phenomenon of dissolution in physiological osseous reconstruction would lead to the invasion of these pores. In the case of powder/grains mixtures, three samples (1–3) prepared with sucrose with the higher granulometry (565 μm) had a mesoporosity c.a. 30%. For the others, mesoporosity increased (20–51%) as the percentage of porogen increased. The lower percentage of mesoporosity (c.a. 20%) was observed with sample 10. In the case of grains/grains mixture, the mesoporosity became high as the granulometry of sucrose granules decreased (from 2 to 25% for sample 13–16) with mesoporosity percentages inferior to 10% for samples 13–15. Mixing powder with sucrose grains resulted in inferior microporosities (12–30%) while mixing apatite grains with sucrose grains gave small values (12–15%). This phenomenon can be easily explained by the fact that the microporosity is created by the interparticular spaces between the apatite particles. In the case of G/G mixing, the apatite was compacted then sintered before its granulation, so the interparticular spaces decreased significantly. When considering that a microporosity of 10% is sufficient to permit the diffusion of the environmental liquid in the total network for the dissolution and precipitation of the material, the best conditions were obtained for samples 3, 9, 12 for P/G mixing on the one hand and for all samples being prepared with the association of G/G (13–16) on the other hand.

5. Conclusion

The goal of the present work which consisted in a control of the porosity repartition in a Ca/P biomaterial was thus achieved. Depending on individual aforementionned factors (porogen, mineral, sintering,...), any material may exhibit perfect porosity properties. We suggest the use of Ca/P materials with total Hg porosity superior to the reference (samples 3 and 6), with higher Hg macroporosity (samples 1–3, 6, 9, 13–16), lower Hg mesoporosity (13–15) and lower Hg microporosity (all samples). Concerning the SEM macroporosity, 10 samples have a higher macroporosity than the reference (3, 5, 6, 8, 9, 12–16). Total porosity analysed by Hg porosimetry being under evaluated, as a consequence of the limit of macropores detection (300 μm), and SEM analyses showing macroporosity of, respectively, 52, 51 and 55% for samples 13–15, it could be deduced that their total porosity was actually higher. The results of the study dealing with a mixing of apatite granules (obtained by crushing and sieving sintered compressed blocks of CDA) with sucrose granules, which favours the best mixing homogeneity and the best repartition of macroporosity, mesoporosity and microporosity is very promising. Further explorations with percentages of sucrose higher than 45% will be necessary to define the limit of sucrose incorporation percentage. Porous structures must be evaluated in terms of resistance to pressure as it is a critical problem that limits clinical applications. The double sintering of CDA in the study consisting in mixing apatite granules to sucrose granules let us think that the obtained blocks will be more resistant. Another study about macroporous interconnections has also been investigated by our team [33]. Preliminary results have shown that interconnections are characterized by permeability and tortuosity and that there is no systematic correlation between the porosity level and the permeability or tortuosity degree. Therefore, a porous ceramic is not necessarily interconnected. Finally, to fully evaluate the effectiveness of the proposed biomaterials, further studies, including *in vivo* experiments, will be required. In this matter, implantations in rabbits have already shown some interesting results [34].

Acknowledgments

The authors are grateful to Mr P. Pilet, ''Service Commun de microscopie Electronique'', Nantes, for his contribution to image analysis, Mr J. Battini ''Micromeritics Society, Verneuil en Halatte, France'', for his help in porosimetry analysis, Mr C. Boiteux for performing the block cutting and Mrs A. Gouyette for her assistance with the porosimetry analyser.

References

[1] G. Daculsi, N. Passuti, Effect of the macroporosity for osseous substitution of calcium phosphate ceramics, Biomaterials 11 (1990) 86–87.
[2] P.S. Eggli, W. Müller, R.K. Schenk, Porous hydroxyapatite and tricalcium phosphate cylinders with two different pore size ranges implanted in the cancellous bone of rabbits. A comparative histomorphometric and histologic study of bony ingrowth and implant substitution, Clinical Orthopaedics 232 (1988) 127–138.

[3] M. Fabbri, G.C. Celotti, A. Ravaglioli, Granulates based on calcium phosphate with controlled morphology and porosity for medical applications: physico-chemical parameters and production technique, Biomaterials 15 (6) (1994) 474–477.
[4] J.M. Bouler, M. Trécant, J. Delecrin, J. Royer, N. Passuti, G. Daculsi, Macroporous biphasic calcium phosphate ceramics: influence of five synthesis parameters on compressive strength, Journal of Biomedical Materials Research 32 (1996) 603–609.
[5] M. Jarcho, Calcium phosphate ceramics as hard tissue prosthetics, Clinical Orthopaedics and Related Research 157 (1981) 259–278.
[6] A. Uchida, S. Nade, E. McCartney, W. Ching, Bone ingrowth into three different porous ceramics implanted into the tibia of rats and rabbits, Journal of Orthopaedic Research 3 (1) (1985) 65–77.
[7] D.M. Liu, Fabrication of hydroxyapatite ceramic with controlled porosity, Journal of Materials Sciences: Materials in Medicine 8 (1997) 227–232.
[8] H.K. Hockin, G. Carl, J.R. Simon, Self hardening calcium phosphate composite scaffold for bone tissue engineering, Journal of Orthopaedic Research 22 (3) (2004) 535–543.
[9] H.R. Lin, Y.J. Yeh, Porous alginate/hydroxyapatite composite scaffolds for bone tissue engineering: preparation, characterization and *in vitro* studies, Journal of Biomedical Material Research Part B: Applied Biomaterial 71B (1) (2004) 52–65.
[10] Y.K. Jun, W.H. Kim, O.K. Kweon, S.H. Hong, The fabrication and biochemical evaluation of alumina reinforced calcium phosphate porous implants, Biomaterials 24 (21) (2003) 3731–3739.
[11] M. Sous, R. Bareille, F. Rouais, D. Clément, J. Amédée, B. Dupuy, C. Baquey, Cellular biocompatibility and resistance to compression of macroporous β-tricalcium phosphate ceramics, Biomaterials 19 (1998) 2147–2153.
[12] J.C. Le Huec, T. Schaeverbeke, D. Clement, J. Faber, A. Le Rebeller, Influence of porosity on the mechanical resistance of hydroxyapatite ceramics under compressive stress, Biomaterials 16 (2) (1995) 113–118.
[13] J.E. Barralet, T. Gaunt, A.J. Wright, R. Gibson, J.C. Knowles, Effect of porosity reduction by compaction on compressive strength and microstructure of calcium phosphate cement, Journal of Biomedical Materials Research 63 (1) (2002) 1–9.
[14] J. Saggio-Woyansky, C.E. Scott, W.P. Minnear, Processing of porous ceramics, American Ceramic Society Bulletin 71 (11) (1992) 1674–1682.
[15] M. Fabbri, G.C. Celloti, A. Ravaglioli, Hydroxyapatite-based porous aggregates: physico-chemical nature, structure, texture and architecture, Biomaterials 16 (3) (1995) 225–228.
[16] C. Wu, J. Chang, W. Zhai, S. Ni, J. Wang, Porous akermanite scaffolds for bone tissue engineering: preparation, characterization and *in vitro* studies, Journal of Biomedical Materials Research Part B: Applied Biomaterials 78B (1) (2006) 47–55.
[17] D.M. Roy, S.K. Linnehan, Hydroxyapatite formed from coral skeletal carbonate by hydrothermal exchange, Nature 247 (1974) 220–222.
[18] W.G. Hubbard, Physiological calcium phosphates as orthopedic biomaterials. Ph D. Thesis, Marquette University, Milwaukee, WI, 1974, 169 pp.
[19] J.X. Lu, B. Flautre, K. Anselme, P. Hardouin, A. Gallur, M. Descamps, B. Thierry, Role of interconnections in porous bioceramics on bone recolonization *in vitro* and *in vivo*, Journal of Materials Sciences: Materials in Medicine 10 (1999) 111–120.
[20] D.M. Liu, Influence of porous microarchitecture on the *in vitro* dissolution and biological behavior of porous calcium phosphate ceramics, Materials Science Forum 250 (1997) 183–208.
[21] L. Olah, K. Filipczak, Z. Jaergermann, T. Czigany, L. Borbas, S. Sosnowski, P. Ulanski, J.M. Rosiak, Synthesis, structural and mechanical properties of porous polymeric scaffolds for bone tissue regeneration bases on neat poly(ε-caprolactone) and its composites with calcium carbonate, Polymers for Advanced Technologies 17 (11–12) (2006) 889–897.
[22] R.M. Pilliar, M.J. Filiagi, J.D. Wells, M.D. Grynpas, R.A. Kandel, Porous calcium polyphosphate scaffolds for bone substitute application—*in vitro* characterization, Biomaterials 22 (9) (2001) 963–972.
[23] A. Slosarczyk, J. Szymura-Oleksiak, B. Mycek, The kinetics of pentoxifylline release from drug-loaded hydroxyapatite implants, Biomaterials 21 (2000) 1215–1221.
[24] I.H. Arita, D.S. Wilkinson, M.A. Mondragon, V.M. Castano, Chemistry and sintering behaviour of thin hydroxyapatite ceramics with controlled porosity, Biomaterials 16 (1995) 403–408.
[25] I.H. Arita, V.M. Castano, D.S. Wilkinson, Synthesis and processing of hydroxyapatite ceramic tapes with controlled porosity, Journal of Materials Sciences: Materials in medicine 6 (1995) 19–23.
[26] O. Gauthier, J.M. Bouler, E. Aguado, P. Pilet, G. Daculsi, Macroporous biphasic calcium phosphate ceramics: Influence of macropore diameter and macroporosity percentage on bone ingrowth, Biomaterials 19 (1–3) (1998) 133–139.
[27] O. Gauthier, E. Goyenvalle, J.M. Bouler, J. Guicheux, P. Pilet, P. Weiss, G. Daculsi, Macroporous biphasic calcium phosphate ceramics versus injectable bone substitute: a comparative study 3 and 8 weeks after implantation in rabbit bone, Journal of Materials Sciences: Materials in Medicine 12 (5) (2001) 385–390.
[28] J.M. Bouler, R.Z. LeGeros, G. Daculsi, Biphasic calcium phosphates: influence of the three synthesis parameters on the HA/β-TCP ratio, Journal of Biomedical Material Research 51 (2000) 680–684.
[29] H. Gautier, C. Merle, J.L. Auget, G. Daculsi, Isostatic compression, a new process for incorporating vancomycin into biphasic calcium phosphate: comparison with a classical method, Biomaterials 21 (3) (2000) 243–249.
[30] K. Ishikawa, P. Ducheyne, S. Radin, Determination of the CA/P ratio in calcium-deficient hydroxyapatite using X-Ray diffraction analysis, Journal of Materials Sciences: Materials in Medicine 4 (1993) 165–168.
[31] J.M. Toth, W.M. Hirthe, W.A. Hubbard, W.A. Brantley, K.L. Lynch, Determination of the ratio of HA/TCP mixtures by X-ray diffraction, Journal of Applied Biomaterials 2 (1991) 37–40.
[32] D. Tadic, M. Epple, Mechanically stable implants of synthetic bone mineral by cold isostatic pressing, Biomaterials 24 (25) (2003) 4565–4571.
[33] A. Lecomte, H. Gautier, J.M. Bouler, A. Gouyette, Y. Pegon, G. Daculsi, C. Merle, Biphasic calcium phosphate: a comparative study of interconnected porosity in two ceramics, Journal of Biomedical Materials Research Part B: Applied Biomaterials 84B (2008) 1–6.
[34] Unpublished results.